Supporting information

High-throughput microwave-assisted discovery of new metal phosphonates

Mark Feyand,[a] Christopher F. Seidler[d], Carsten Deiter,[b] Andre Rothkirch,[b] Alexandra Lieb[c], Michael Wark[d] and Norbert Stock[a,*]

a Institut für Anorganische Chemie, Christian-Albrechts-Universität, Max-Eyth Straße 2, 24118 Kiel, Germany E-mail: stock@ac.uni-kiel.de

b HASYLAB, DESY Hamburg, Notkestraße 85, 22607 Hamburg, Germany.

c Institut für Chemie, Otto von Guericke Universität, Universitätsplatz 2, 39106, Magdeburg, Germany.

d Lehrstuhl für Technische Chemie, Ruhr-Universität Bochum, Universitätsstr. 150, D44801, Bochum, Germany.

NMR SPECTROSCOPY

a) *p*-$(H_2O_3PCH_2)_2N{-}C_6H_4{-}N(CH_2PO_3H_2)_2$ (*p*-H_8L)

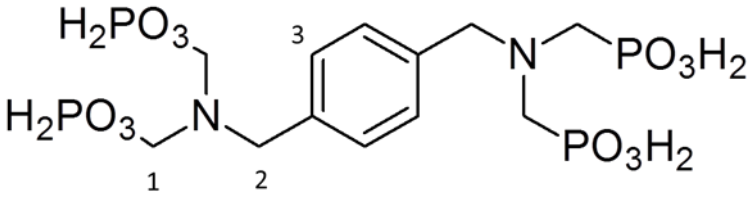

^{1}H-NMR (500 MHz, NaOD/D_2O 10 %, TMS): = 7.11 (s, 4H, C3-H), 3.54 (s, 4H, C2-H), 2.34 (d, 8H, $^3J_{P\text{-}H}$ = 11.8 Hz, C1-H) ppm.
^{31}P-NMR (500 MHz, NaOD/D_2O 10 %, H_3PO_4): = 17.06 ppm (s).

b) *m*-$(H_2O_3PCH_2)_2N{-}C_6H_4{-}N(CH_2PO_3H_2)_2$ (*m*-H_8L)

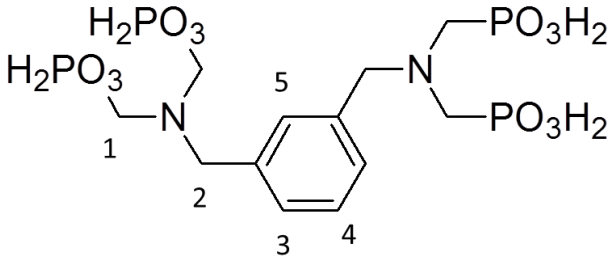

^{1}H-NMR (500 MHz, NaOD/D2O 10 %, TMS): = 6.80-6.70 (s, 4H, C3-H,C4-H,C5-H), 3.24 (s, 4H, C2–H), 1.90 (d, 8H, $^3J_{P\text{-}H}$ = 11.5 Hz, C1–H) ppm.
^{31}P-NMR (500 MHz, NaOD/D2O 10 %, H_3PO_4): = 17.06 ppm (s).

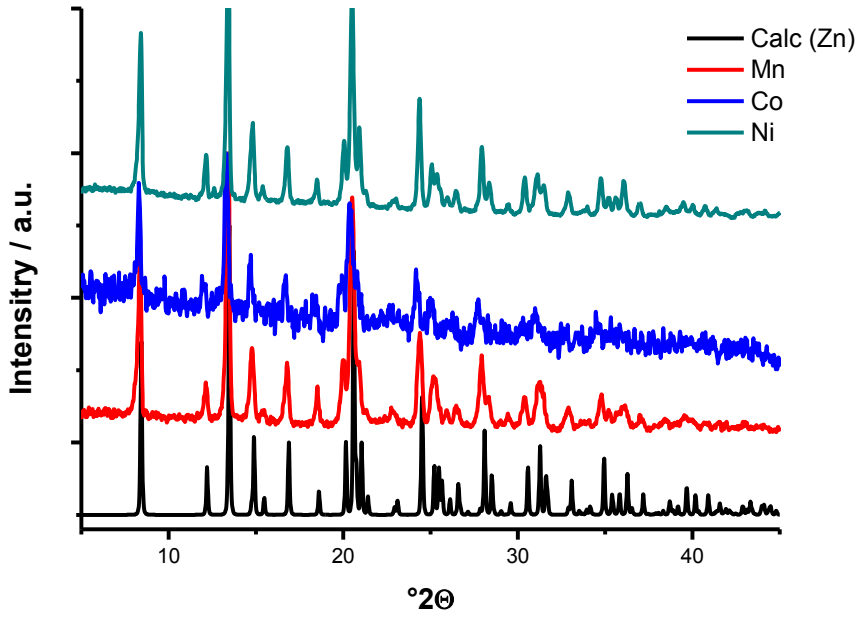

Fig. S2 X-ray powder diffraction patterns of M[*p*-$(HO_3PCH_2)_2N(H)$-CH_2-C_6H_4-CH_2-$N(H)(CH_2PO_3H)_2(H_2O)$] (M= Mn^{2+}, Co^{2+}, Ni^{2+}) (**2**). The structure determination was carried out using XRD pattern of **2** (Zn).

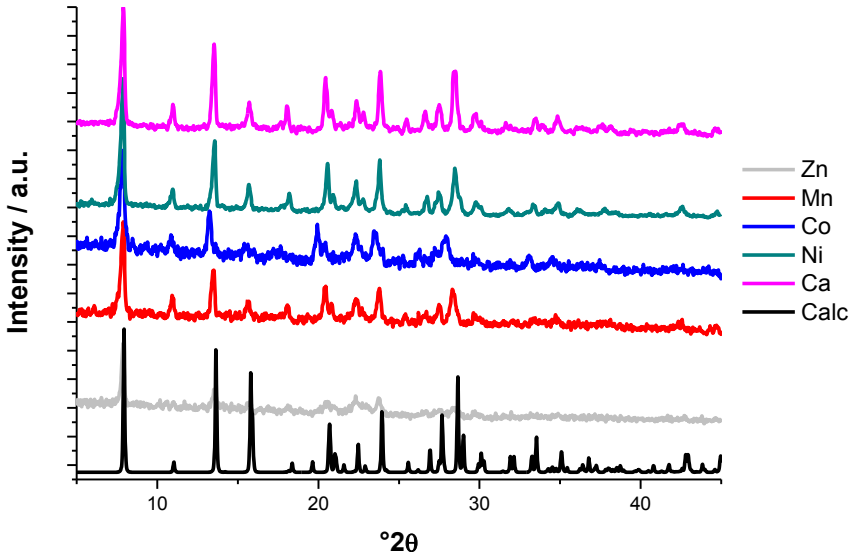

Fig. S3 X-ray powder diffraction patterns of M[*m*-$(HO_3PCH_2)_2N(H)$-CH_2-C_6H_4-CH_2-$N(H)(CH_2PO_3H)_2$] (H_2O) (M= Ca^{2+}, Mn^{2+}, Co^{2+}, Ni^{2+}, Zn^{2+}) (**3**). The calculated powder pattern is shown in black below. The structure determination was carried out using XRD pattern of **3** (Ni).

Exact reaction condition

Table S1. Exact amounts of the educts used in the high-throughput reactions.The following metal salts were used: $Ca(NO_3)_2{\cdot}4H_2O$, $Mn(NO_3)_2{\cdot}6H_2O$, $Co(NO_3)_2{\cdot}6H_2O$, $Ni(NO_3)_2{\cdot}6H_2O$, $Zn(NO_3)_2{\cdot}6H_2O$, $Cd(NO_3)_2{\cdot}4H_2O$, $CaCl_2{\cdot}4H_2O$, $MnCl_2{\cdot}2H_2O$, $CoCl_2{\cdot}2H_2O$, $NiCl_2{\cdot}6H_2O$, $ZnCl_2$, $CdCl_2$

Metall	Counterion	Nr.	H_8L	M		H_8L [mg]	H_2O [µl]	2M M^{2+} [µl]	Nr.	Result (identified by XRPD)
Ca^{2+}	NO_3^{2-}	1	1	1		50	2000	49	1	X-ray amorphous
Mn^{2+}	NO_3^{2-}	2	1	1		50	2000	49	2	X-ray amorphous
Co^{2+}	NO_3^{2-}	3	1	1	R	50	2000	49	3	X-ray amorphous
Ni^{2+}	NO_3^{2-}	4	1	1	1	50	2000	49	4	X-ray amorphous
Zn^{2+}	NO_3^{2-}	5	1	1		50	2000	49	5	X-ray amorphous
Cd^{2+}	NO_3^{2-}	6	1	1	1	50	2000	49	6	1
Ca^{2+}	Cl^-	7	1	1		50	2000	49	7	$[Ca(p\text{-}H_6L)]{\cdot}2H_2O$ [1]
Mn^{2+}	Cl^-	8	1	1		50	2000	49	8	2
Co^{2+}	Cl^-	9	1	1	R	50	2000	49	9	2
Ni^{2+}	Cl^-	10	1	1	2	50	2000	49	10	2
Zn^{2+}	Cl^-	11	1	1		50	2000	49	11	2
Cd^{2+}	Cl^-	12	1	1		50	2000	49	12	X-ray amorphous
Ca^{2+}	NO_3^{2-}	13	1	1		50	2000	49	13	3
Mn^{2+}	NO_3^{2-}	14	1	1		50	2000	49	14	3
Co^{2+}	NO_3^{2-}	15	1	1	R	50	2000	49	15	3
Ni^{2+}	NO_3^{2-}	16	1	1	3	50	2000	49	16	3
Zn^{2+}	NO_3^{2-}	17	1	1		50	2000	49	17	3
Cd^{2+}	NO_3^{2-}	18	1	1		50	2000	49	18	X-ray amorphous
Ca^{2+}	Cl^-	19	1	1		50	2000	49	19	X-ray amorphous
Mn^{2+}	Cl^-	20	1	1		50	2000	49	20	X-ray amorphous
Co^{2+}	Cl^-	21	1	1	R	50	2000	49	21	X-ray amorphous
Ni^{2+}	Cl^-	22	1	1	4	50	2000	49	22	X-ray amorphous
Zn^{2+}	Cl^-	23	1	1		50	2000	49	23	X-ray amorphous
Cd^{2+}	Cl^-	24	1	1		50	2000	49	24	X-ray amorphous

STRUCTURE DETERMINATION OF 2.

The crystal structure was solved by molecular modeling techniques using Materials Studio 5.5. The results of the elemental analysis and the indexing procedure need to be taken into account. The elemental analysis lead to the molar ratio Zn^{2+} : linker = 1 : 1. Taking the unit cell volume of 527 $Å^3$ into account and a volume of 18 $Å^3$ per non-hydrogen atom only 30 non-hydrogen atoms fit into the unit cell. According to the chemical formula only one Zn^{2+} ion and one tetraphosponate linker molecule can be present in the unit cell. Thus, in the space group *P*-1 the Zn ion and the linker must be located on special positions. The, for developing the structural model, important inversion centers in the space group *P*-1 are given in Figure 3 (top). The Zn ion was placed on 0.5/0.5/0.5 and the phenyl ring around 0/0/0 as shown in Figure 3 middle. The phenyl ring was connected by the CH_2-NH-(CH_2-PO_3H^-)$_2$ groups with the Zn ion and the coordination sphere was completed by adding a water molecule (Figure 3 bottom). The obtained model was used for further Rietveld refinements.

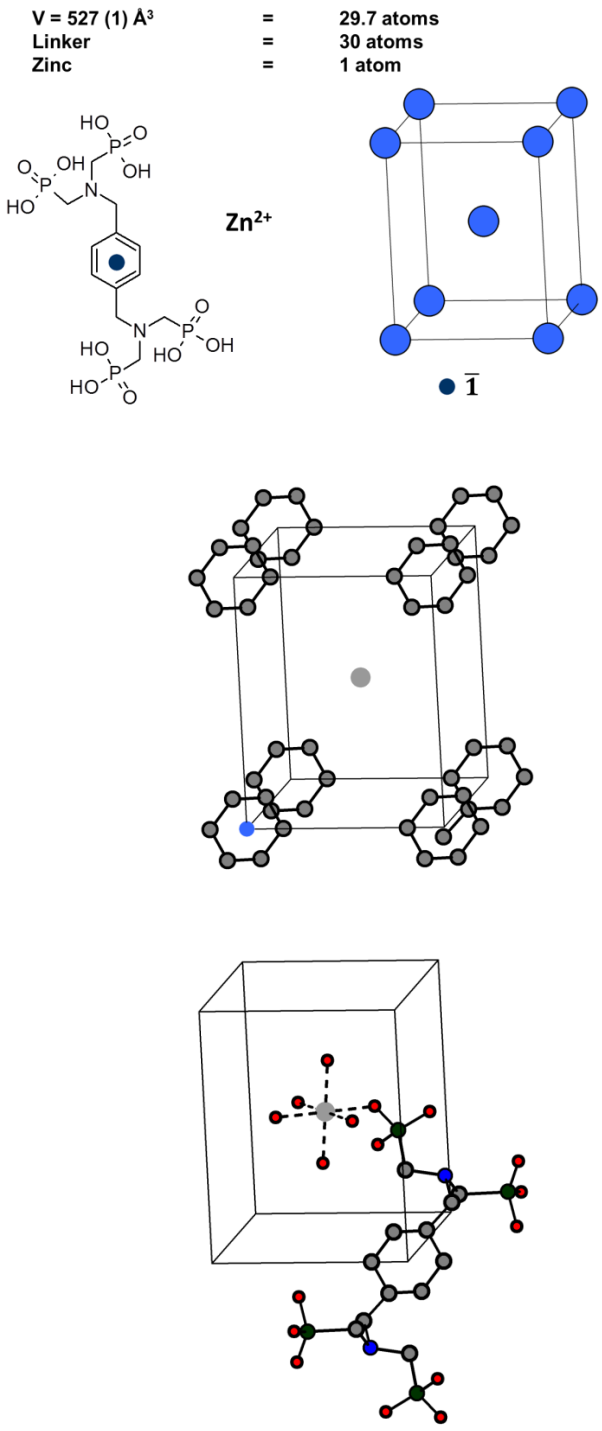

Fig. S4. Important inversion centers in the space group P-1 for deriving the structural model and the inversion center of the linker molecule (top); Initial model by placing the phenylring and the Zn ion on/ around the inversion center (middle) and final starting model for the Rietveld refinement (bottom).

CRYSTAL STRUCTURES

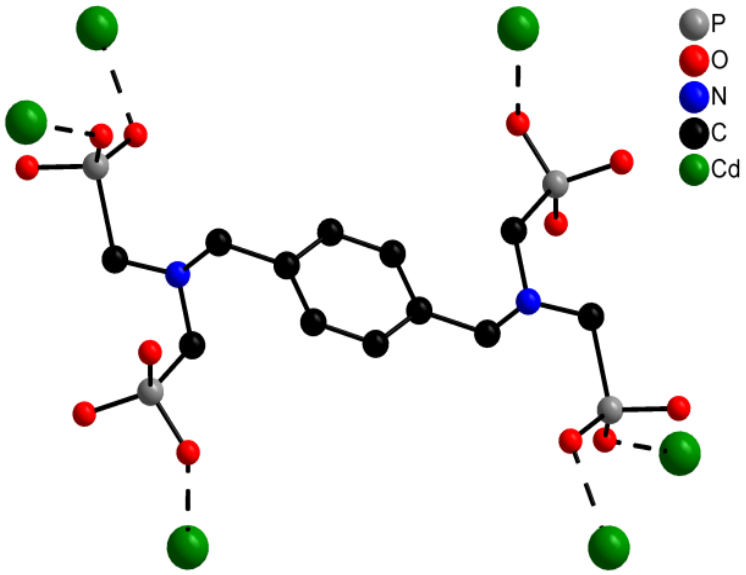

Fig. S5. Interconnection of the Cd^{2+} ions by the linker molecule in the structure of Cd[*p*-$(HO_3PCH_2)_2N(H)$-CH_2-C_6H_4-CH_2-$N(H)(CH_2PO_3H)_2$] (**1**). Fragmented lines represent Cd-O bonds.

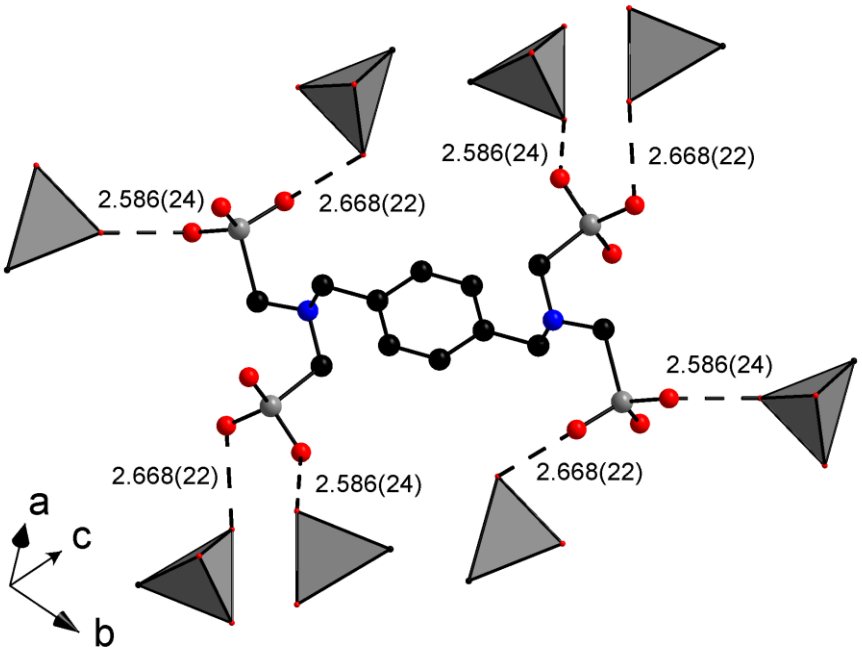

Fig. S6. Hydrogen bonds of the phosphonate groups in compound of Cd[*p*-$(HO_3PCH_2)_2N(H)$-CH_2-C_6H_4-CH_2-$N(H)(CH_2PO_3H)_2$] (**1**) and their bond lengths.

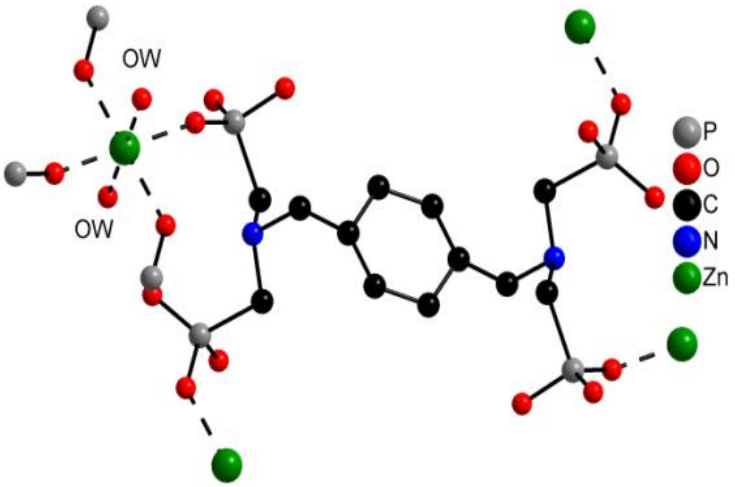

Fig. S7. Interconnection of the metal ions by the linker molecules in the structure of M[*p*-$(HO_3PCH_2)_2N(H)$-CH_2-C_6H_4-CH_2-$N(H)(CH_2PO_3H)_2(H_2O)$] (M=Ca, Mn, Co , Ni, Zn) ***(2)*** Fragmented lines represent M-O bonds.

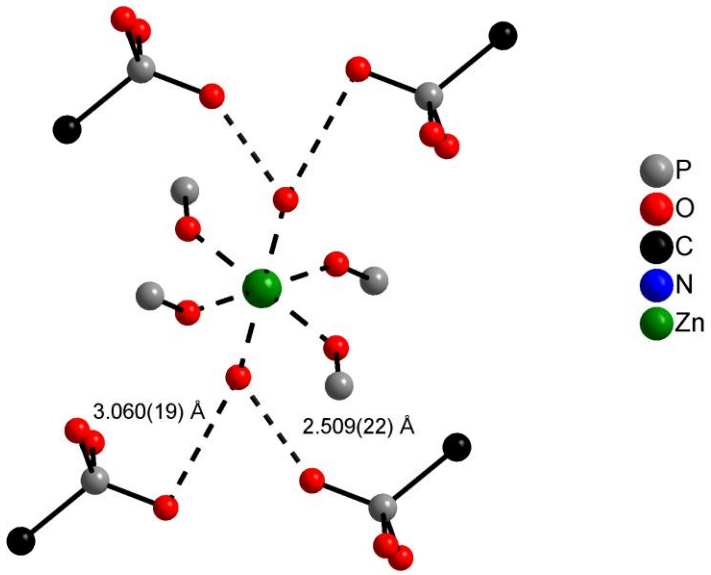

Fig. S8. Possible hydrogen bonds of the coordinated water molecule in the structure of Zn[*p*-$(HO_3PCH_2)_2N(H)$-CH_2-C_6H_4-CH_2-$N(H)(CH_2PO_3H)_2(H_2O)$] ***(2)***

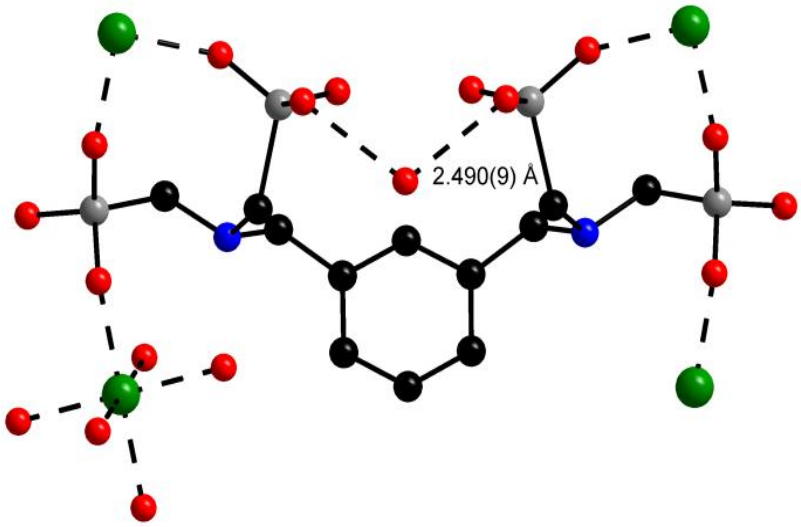

Fig. S9. Interconnection of the metal ions by the linker molecule and possible hydrogen bonds of the water molecule in the structure of M[*m*-$(HO_3PCH_2)_2$N(H)-CH_2-C_6H_4-CH_2-N(H)$(CH_2PO_3H)_2$]·H_2O (M=Ca, Mn, Co, Ni, Zn) (**3**).

IR SPECTROSCOPY

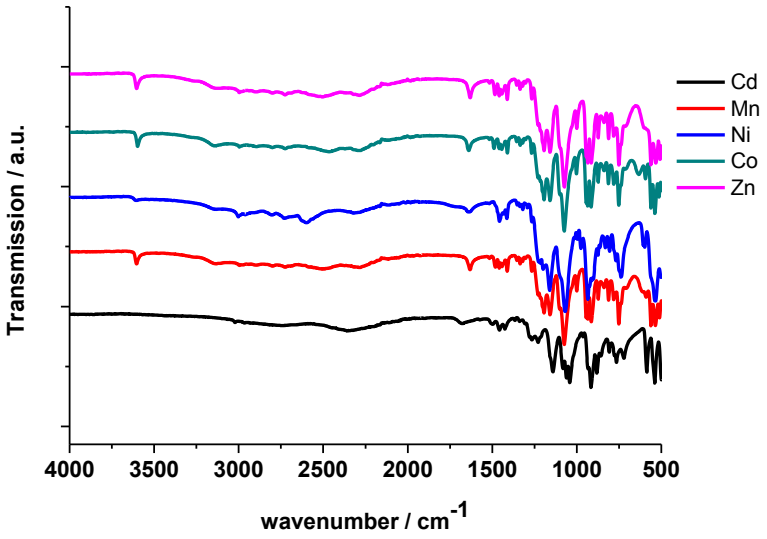

Fig. S10. IR spectra of the title compounds M[*p*-$(HO_3PCH_2)_2N(H)$-CH_2-C_6H_4-CH_2-$N(H)(CH_2PO_3H)_2(H_2O)$] (M=Cd, Mn, Co , Ni, Zn) ***(1,2.)***

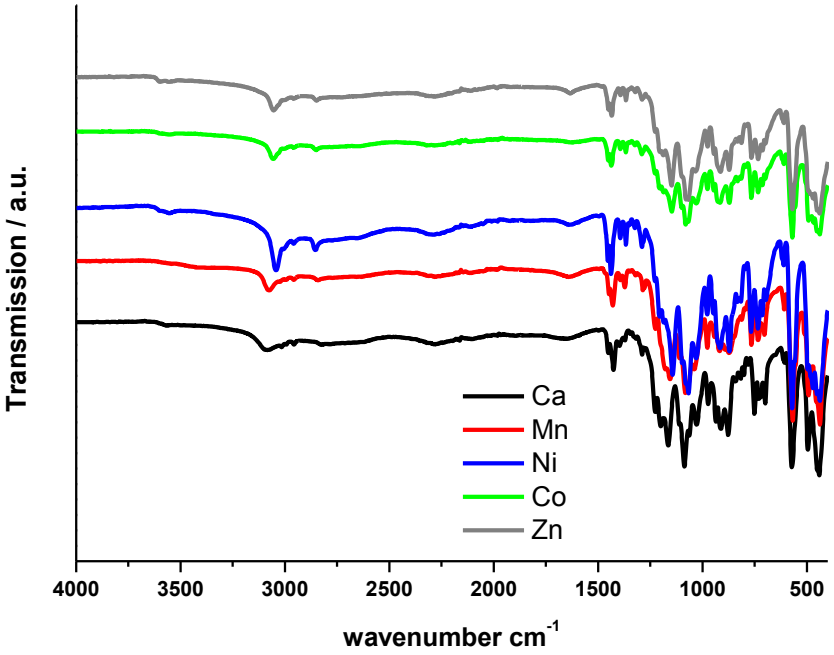

Fig. S11. IR spectra of the title compounds M[*m*-$(HO_3PCH_2)_2N(H)$-CH_2-C_6H_4-CH_2-$N(H)(CH_2PO_3H)_2$]·H_2O (M=Ca, Mn, Co, Ni, Zn) (**3**).

THERMOGRAVIMETRIC ANALYSE

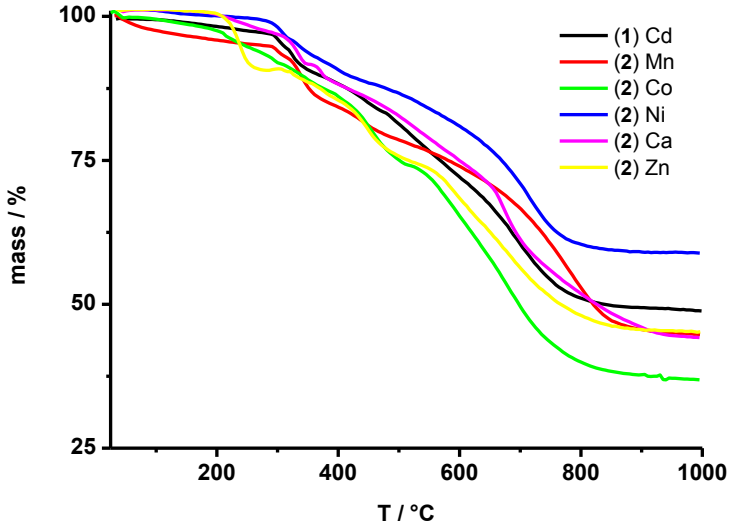

Fig. S12. Results of the thermogravimetric analyses of M[*p*-$(HO_3PCH_2)_2N(H)$-CH_2-C_6H_4-CH_2-$N(H)(CH_2PO_3H)_2(H_2O)$] (M=Cd, Ca, Mn, Co , Ni, Zn) (**1,2**).

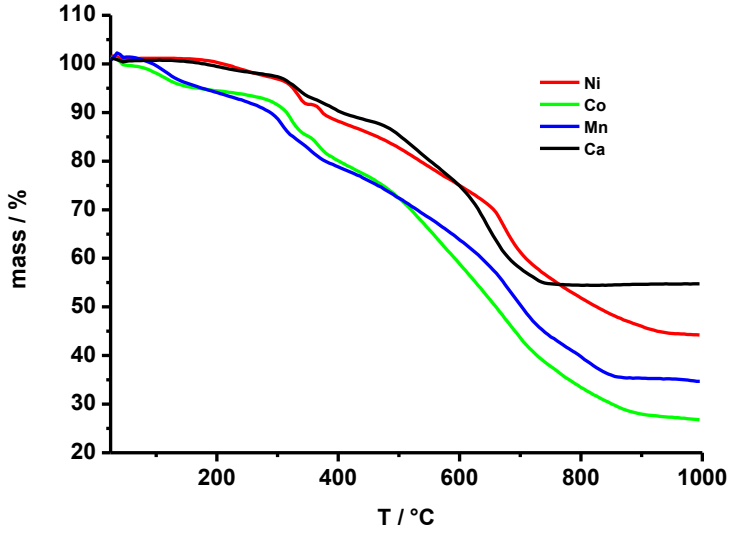

Fig. S13. Results of the thermogravimetric analyses of M[*m*-$(HO_3PCH_2)_2N(H)$-CH_2-C_6H_4-CH_2-$N(H)(CH_2PO_3H)_2$]·H_2O (M=Ca, Mn, Co, Ni, Zn) (**3**).

PROTON CONDUCTIVITY

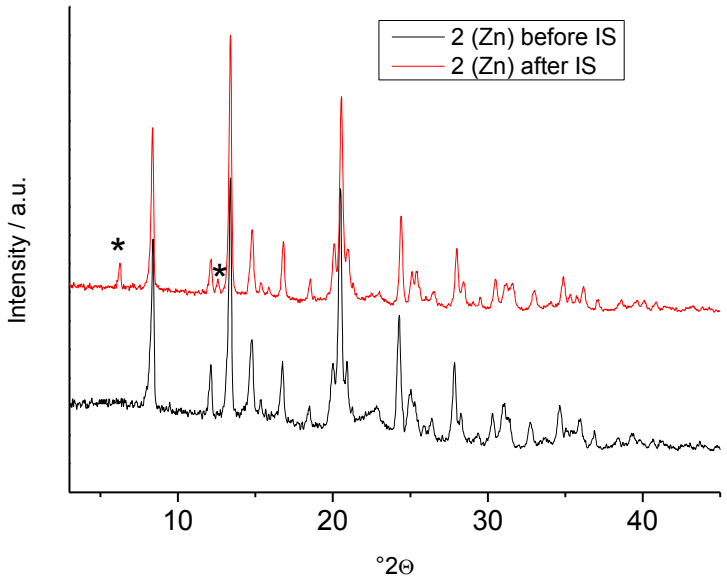

Fig. S14 . X-ray powder patterns before (black) and after (red) impedance spectroscopy measurements of **2** (Zn). The impurities are marked with a star.

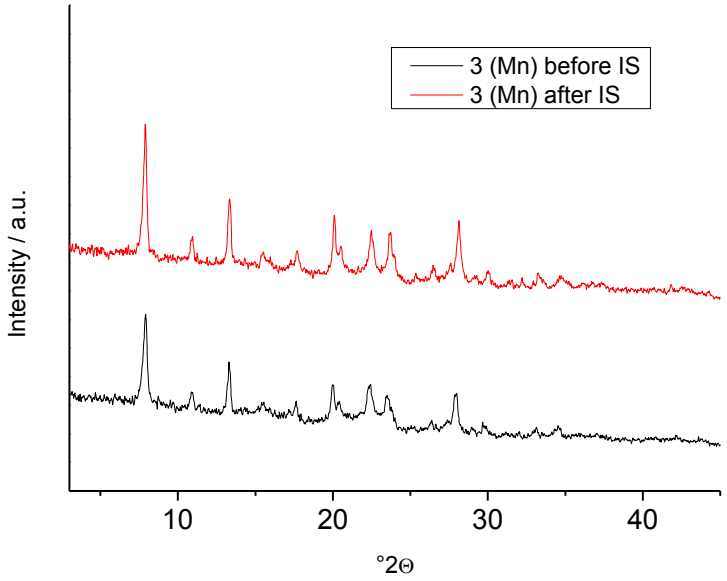

Fig. S15 . X-ray powder patterns before (black) and after (red) impedance spectroscopy measurements of 3 (Mn).

LITERATURE

1. *Stock, N.; Stoll, A.; Bein, T., Microporous and Mesoporous Materials* ***2004,*** *69 (1–2), 65.*